Porous Materials

DOI: 10.1002/anie.201200024

Carbide-Derived Carbon Monoliths with Hierarchical Pore Architectures**

*Martin Oschatz, Lars Borchardt, Matthias Thommes, Katie A. Cychosz, Irena Senkovska, Nicole Klein, Robert Frind, Matthias Leistner, Volker Presser, Yury Gogotsi, and Stefan Kaskel**

Porous carbon materials are crucial components in catalysis,[1] gas storage,[2] electronics,[3] and biochemistry.[4] A hierarchical pore architecture in these materials is essential to achieve high surface areas combined with advanced mass transport kinetics.[5] Widely used approaches for the generation of micro- or mesopores are activation[6] and nanocasting.[7] In contrast, macroporous carbon materials are primarily obtained by carbonization of polymeric precursor gels[8] or replication of larger templates.[9]

A relatively new class of micro- and mesoporous carbon material with tunable porosity are carbide-derived carbon materials (CDCs).[10] High-temperature chlorination of carbides leads to selective removal of metal- or semi-metal atoms and allows control over the pore size of the resulting CDCs in a sub-Ångström range by changing synthesis conditions or the carbide precursor.[11] These materials have been studied for applications in gas storage[12] and as electrode materials in supercapacitors because of their high specific surface areas.[13]

Recently, metal etching from pyrolyzed pre-ceramic components (polysilsesquioxanes or polysilazanes) was found to be a useful route towards carbide-derived carbon materials with enhanced porosity and gas-storage properties.[14,15] A significant step towards ultrahigh specific surface area combined with a hierarchical mesoporous–microporous system was achieved using nanocasting of silica templates (SBA-15[16] or KIT-6[17]) with polycarbosilane precursors and subsequent chlorine treatment of the resulting ordered mesoporous silicon carbides.[18] These ordered mesoporous CDCs offer specific surface areas as high as 2800 $m^2 g^{-1}$ and total pore volumes of up to 2 $cm^3 g^{-1}$. Their mesostructure can be easily controlled by changing the silica hard template,[19] resulting in excellent performance in protein adsorption,[18] gas storage,[19,20] and as electrodes for supercapacitors.[19,21] However, such carbon materials are available only as non-structured micrometer-sized powders and cannot be shaped into films without the addition of binders or the use of high mechanical stress, leading to structural deformation.

Chlorine treatment of mechanically mixed Si/SiC precursors was found to be a useful route towards monolithic CDC with a hierarchical pore system. The presence of a free metal phase in the precursor system provides the opportunity to introduce a secondary macroporosity of 3 μm sized channels with a volume of 0.23 $cm^3 g^{-1}$ along with the microporous carbide-derived carbon material system.[22]

The introduction of large transport pores in polymer-based CDCs might be an alternative way to form materials that combine high surface areas with efficient fluid transport. The current literature describes a variety of routes for the production of highly macroporous ceramics from precursor polymers with controllable cell and window sizes.[23] In particular, direct blowing of polycarbosilanes was found to be a useful approach for the generation of silicon carbide foams that might be suitable materials for the production of hierarchical CDCs.[24]

In the following, we describe a novel synthesis route for monolithic carbide-derived carbon materials, including micro-, meso-, and macroporous structures with extremely high specific surface area. They can be obtained by high-temperature chlorination of macroporous polymer-derived silicon carbide (SiC-PolyHIPE).[25] A soft-templating approach starting from a high internal phase emulsion (HIPE)[26] was used with an external oil phase consisting of liquid polycarbosilane SMP-10 and the cross-linker *para*-divinylbenzene. Using Span-80 as surfactant to stabilize the internal water phase, the application of oxidic or carbon hard templates and the corresponding template removal under harsh conditions is no longer necessary. After cross-linking the polymer chains, the resulting PolyHIPEs were pyrolyzed to silicon carbides at maximum temperatures of 700, 800, and 1000 °C and subsequently converted into CDCs by chlorine treatment at the maximum pyrolysis temperature (Supporting

[*] M. Oschatz, L. Borchardt, Dr. I. Senkovska, N. Klein, Dr. R. Frind, Prof. Dr. S. Kaskel
Department of Inorganic Chemistry
Dresden University of Technology
Bergstrasse 66, 01062 Dresden (Germany)
E-mail: stefan.kaskel@chemie.tu-dresden.de
Dr. M. Thommes, Dr. K. A. Cychosz
Quantachrome Instruments
1900 Corporate Drive, Boynton Beach, FL 33426 (USA)
M. Leistner, Prof. Dr. S. Kaskel
Fraunhofer Institute for Material and Beam Technology
Winterbergstrasse 28, 01277 Dresden (Germany)
Dr. V. Presser
INM—Leibniz Institute for New Materials
Campus D2 2, 66123 Saarbrücken (Germany)
Prof. Dr. Y. Gogotsi
Department of Materials Science and Engineering
A. J. Drexel Nanotechnology Institute
3141 Chestnut Street, Philadelphia, PA 19104 (USA)

[**] This work was financially supported by the German Research Foundation (SPP 1181 NANOMAT). We also thank the DAAD for financial support. Y.G. and V.P. gratefully acknowledge the support of the U.S. Department of Energy/Office of Electricity's Energy Storage Program.

Supporting information for this article (detailed information about DUT-38 synthesis, adsorption measurements, and characterization) is available on the WWW under http://dx.doi.org/10.1002/anie.201200024.

Information, Scheme S1). A subsequent reductive treatment under flowing hydrogen was performed to ensure the removal of all residual chlorine and metal chlorides adsorbed in the pores of the CDC products (in the following designated as DUT-38; DUT = Dresden University of Technology; Supporting Information, Table S1). The monolithic morphology of the PolyHIPEs can be fully maintained over the entire synthesis pathway (Supporting Information, Figure S1). Owing to the high surface area combined with the precisely defined macropore arrangements, DUT-38 materials promise excellent capacities in gas storage applications in combination with advanced materials transport.

SEM micrographs of the obtained CDCs (Figure 1; Supporting Information, Figure S1) clearly indicate the presence of a macroporous network that is typical for

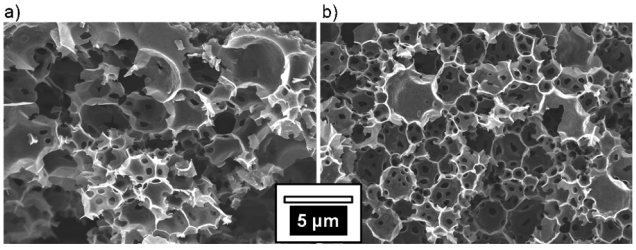

Figure 1. SEM micrographs of DUT-38 prepared at a) 700 °C and b) 800 °C.

PolyHIPEs consisting of large pores (voids) in the micrometer range. They are interconnected by smaller gates (windows) of several 100 nm in diameter. SEM images of the silicon carbide precursors (Supporting Information, Figure S2) show the same morphology, indicating that chlorine treatment is fully conformal and does not deteriorate the macrostructure.

Raman spectra of DUT-38 materials (Figure 2) are comparable with those originally reported for microporous CDC materials.[10] A sharp increase of I_D/I_G ratio can be observed when the synthesis temperature rises from 700 °C to 1000 °C owing to the formation of graphitic carbon and increased structural ordering. The decreasing full-width at half-maximum (FWHM) of the D band as well as the

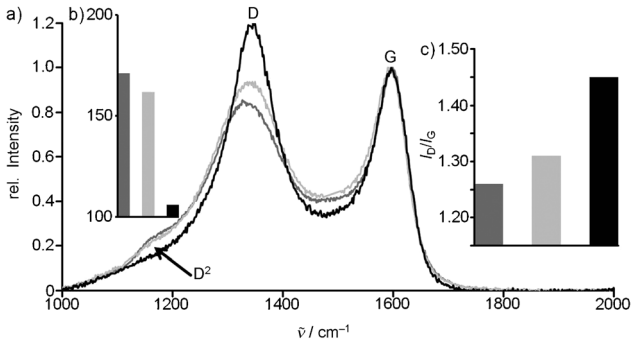

Figure 2. a) Raman spectra, b) full-width at half-maximum (FWHM) of the D band, and c) I_D/I_G ratio of DUT-38 prepared at 700 °C (dark gray), 800 °C (light gray), and 1000 °C (black).

disappearance of the shoulder D^2 band also indicate increased graphitization in the CDCs prepared at higher temperatures.

Nitrogen physisorption measurements (Figure 3; Supporting Information, Table S2) were performed to characterize the micro- and mesopore volumes of the CDCs. The semi-

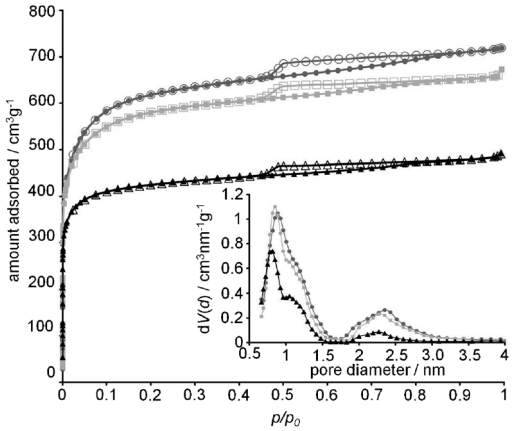

Figure 3. Nitrogen physisorption isotherms (77 K) of DUT-38 prepared at 700 °C (circles), 800 °C (squares), and 1000 °C (triangles). Filled symbols represent the adsorption branch, empty symbols the corresponding desorption. Inset: Corresponding pore size distributions.

logarithmic plots of the isotherms (Supporting Information, Figure S3) highlight the adsorption in the low-pressure regime associated with the filling of narrow micropores. BET surface areas of 2345, 2201, and 1649 $m^2 g^{-1}$ and total pore volumes of 1.1, 1.03, and 0.74 $cm^3 g^{-1}$ were achieved at synthesis temperatures of 700, 800, and 1000 °C, respectively. The decreasing surface areas and pore volumes are related to the preferred formation of graphitic carbon (Figure 2) and structural deformations at higher synthesis temperatures. Even though the walls of DUT-38 carbon materials predominantly contain micropores, the nitrogen adsorption isotherms show hysteresis loops of type H4, indicating the presence of some disordered mesopores. The step in the desorption branches at relative pressures of 0.4–0.5 is caused by cavitation (related to the classical tensile strength effect) in the carbon materials, showing that some of the mesopores are accessible only through the micropores.[27] As the pores do not empty under equilibrium conditions, the pore-size distributions were calculated from the adsorption branches of the isotherms using a method which takes into account the delay in condensation owing to metastable adsorption states. As suggested from the shape of the isotherms, the pore-size distributions show the presence of both micro- and mesopores, with maxima in the diameter ranges of 0.8–0.9 and 2.2–2.3 nm, respectively. Good agreements are observed between the quenched solid density functional theory (QSDFT) fits (carbon slit/cylindrical adsorption branch kernel)[28,29] and the experimental data for all samples (Supporting Information, Figure S4), indicating that this QSDFT carbon kernel gives reliable pore-size distributions.

The strongly interconnected macropore arrangements of DUT-38 yield extraordinary high intrinsic pore volumes on

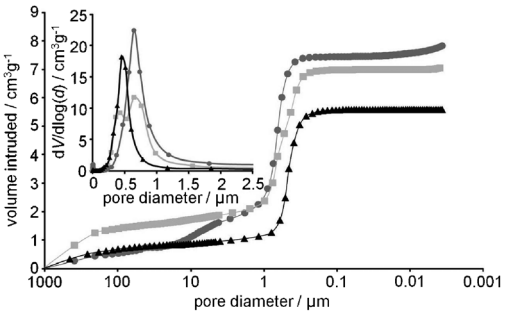

Figure 4. Mercury intrusion curves of DUT-38 prepared at 700 °C (circles), 800 °C (squares), and 1000 °C (triangles). Inset: Corresponding macropore size distributions.

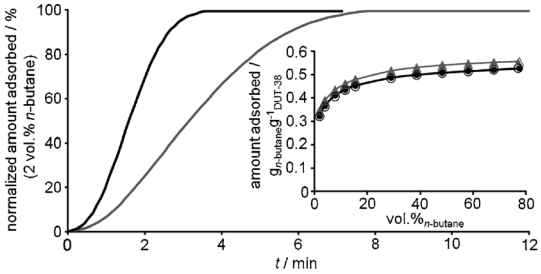

Figure 5. *n*-Butane adsorption kinetic curves of DUT-38 (black) and the microporous CDC reference (gray) at 2 vol.% *n*-butane. Inset: *n*-Butane adsorption isotherms (298 K). Filled symbols represent the adsorption branch, empty symbols the corresponding desorption.

the macroscopic scale (> 50 nm in diameter) of up to 7.45 $cm^3 g^{-1}$, as determined by mercury intrusion porosimetry (Figure 4; Supporting Information, Table S2).

With increasing synthesis temperature, the macropore volumes decrease owing to a higher level of volume shrinkage from PolyHIPEs to silicon carbides. Size distributions of macropores (calculated using the Washburn equation) with maxima in the range of 0.45 to 0.65 µm correspond to the average size of the windows between the larger voids. The diameter of the windows decreases at higher synthesis temperatures, which is again caused by the larger degree of volume shrinkage compared to lower synthesis temperatures. It should be noted that at 700 °C, a rather narrow cell window size distribution centered at 0.65 µm is obtained, while at 1000 °C, the maximum shifts to a value of 0.45 µm in diameter.

Owing to the simultaneous presence of micro- and mesopores in the walls of the original HIPE structure, DUT-38 is a promising material for gas storage and toxic vapor removal (Supporting Information, Table S3, Figures S5–S7). The maximum gravimetric capacity values are 0.18 $g g^{-1}$ methane (excess, 298 K), 0.046 $g g^{-1}$ hydrogen (excess, 77 K), and 0.53 $g g^{-1}$ *n*-butane (298 K). Moreover, the macropore system should lead to enhanced adsorption kinetics, which is a crucial parameter especially in filter media or membranes.

A comparison of *n*-butane adsorption performances between DUT-38 synthesized at 700 °C and a microporous CDC reference material ("CDC-Micro"; Supporting Information, Figure S8, Table S4) shows quite similar adsorption isotherms (Figure 5, inset), which is due to comparable surface areas and micropore volumes. The major difference between both materials is the absence of a macropore system in the non-foamed reference structure (Supporting Information, Figure S9). However, the adsorption rate at 2 % v/v *n*-butane is significantly higher for the macroporous DUT-38 (Figure 5). The equilibration time to reach full capacity is remarkably reduced owing to the macropore system, leading to superior accessibility of the micropores where the adsorption mainly takes place.

In conclusion, we have presented a novel pathway for the synthesis of monolithic CDCs (DUT-38) that contain pores that range in size from micro- over meso- and up to macropores. Specific surface areas exceeding 2300 $m^2 g^{-1}$ and total micro- and mesopore volumes of up to 1.1 $cm^3 g^{-1}$ are obtained. The materials can be manufactured with complex shapes in a casting approach. Extremely high macropore volumes of up to 7.45 $cm^3 g^{-1}$ render the materials as being highly accessible for larger molecules with high adsorption rates. The hierarchical pore structure is controllable using a soft-templating approach followed by chlorine etching, resulting in excellent capacities and kinetics in gas storage. DUT-38 is also a promising electrode material for electric energy storage devices, capacitive deionization, and whenever high reaction or adsorption rates are required.

Received: January 2, 2012
Revised: March 1, 2012
Published online: June 13, 2012

Keywords: adsorption · carbon · hierarchical structures · porous materials · polyHIPEs

[1] a) R. Schloegl in *Handbook of Heterogeneous Catalysis*, *Vol. 1* (Eds.: G. Ertl, H. Knözinger, F. Schüth, J. Weitkamp), Wiley-VCH, Weinheim, **2008**, pp. 357–427; b) A. Taguchi, F. Schüth, *Microporous Mesoporous Mater.* **2005**, *77*, 1.
[2] a) L. Schlapbach, A. Zuettel, *Nature* **2001**, *414*, 353; b) R. E. Morris, P. S. Wheatley, *Angew. Chem.* **2008**, *120*, 5044; *Angew. Chem. Int. Ed.* **2008**, *47*, 4966.
[3] a) X. Ji, K. T. Lee, L. F. Nazar, *Nat. Mater.* **2009**, *8*, 500; b) J. Chmiola, C. Largeot, P.-L. Taberna, P. Simon, Y. Gogotsi, *Angew. Chem.* **2008**, *120*, 3440; *Angew. Chem. Int. Ed.* **2008**, *47*, 3392.
[4] G. Yushin, E. N. Hoffman, M. W. Barsoum, Y. Gogotsi, C. A. Howell, S. R. Sandeman, G. J. Phillips, A. W. Lloyd, S. V. Mikhalovsky, *Biomaterials* **2006**, *27*, 5755.
[5] J. Lee, J. Kim, T. Hyeon, *Adv. Mater.* **2006**, *18*, 2073.
[6] a) F. Rodríguez-Reinoso, M. Molina-Sabio, M. T. González, *Carbon* **1995**, *33*, 15; b) D. Lozano-Castelló, M. A. Lillo-Ródenas, D. Cazorla-Amorós, A. Linares-Solano, *Carbon* **2001**, *39*, 741.
[7] a) A.-H. Lu, F. Schüth, *Adv. Mater.* **2006**, *18*, 1793; b) S. Jun, S. H. Joo, R. Ryoo, M. Kruk, M. Jaroniec, Z. Liu, T. Ohsuna, O. Terasaki, *J. Am. Chem. Soc.* **2000**, *122*, 10712.
[8] G. Hasegawa, K. Kanamori, K. Nakanishi, T. Hanada, *Carbon* **2010**, *48*, 1757.
[9] S.-W. Woo, K. Dokko, H. Nakano, K. Kanamura, *J. Mater. Chem.* **2008**, *18*, 1674.
[10] V. Presser, M. Heon, Y. Gogotsi, *Adv. Funct. Mater.* **2011**, *21*, 810.

[11] a) R. K. Dash, A. Nikitin, Y. Gogotsi, *Microporous Mesoporous Mater.* **2004**, *72*, 203; b) R. K. Dash, G. Yushin, Y. Gogotsi, *Microporous Mesoporous Mater.* **2005**, *86*, 50.
[12] Y. Gogotsi, R. K. Dash, G. Yushin, T. Yildirim, G. Laudisio, J. E. Fischer, *J. Am. Chem. Soc.* **2005**, *127*, 16006.
[13] J. Chmiola, G. Yushin, Y. Gogotsi, C. Portet, P. Simon, P. L. Taberna, *Science* **2006**, *313*, 1760.
[14] C. Vakifahmetoglu, V. Presser, S.-H. Yeon, P. Colombo, Y. Gogotsi, *Microporous Mesoporous Mater.* **2011**, *144*, 105.
[15] S.-H. Yeon, P. Reddington, Y. Gogotsi, J. E. Fischer, C. Vakifahmetoglu, P. Colombo, *Carbon* **2010**, *48*, 201.
[16] D. Zhao, J. Feng, Q. Huo, N. Melosh, G. H. Frederickson, B. F. Chmelka, G. D. Stucky, *Science* **1998**, *279*, 548.
[17] F. Kleitz, S. H. Choi, R. Ryoo, *Chem. Commun.* **2003**, 2136.
[18] P. Krawiec, E. Kockrick, L. Borchardt, D. Geiger, A. Corma, S. Kaskel, *J. Phys. Chem. C* **2009**, *113*, 7755.
[19] M. Oschatz, E. Kockrick, M. Rose, L. Borchardt, N. Klein, I. Senkovska, T. Freudenberg, Y. Korenblit, G. Yushin, S. Kaskel, *Carbon* **2010**, *48*, 3987.
[20] E. Kockrick, C. Schrage, L. Borchardt, N. Klein, M. Rose, I. Senkovska, S. Kaskel, *Carbon* **2010**, *48*, 1707.
[21] a) Y. Korenblit, M. Rose, E. Kockrick, L. Borchardt, A. Kvit, S. Kaskel, G. Yushin, *ACS Nano* **2010**, *4*, 1337; b) M. Rose, Y. Korenblit, E. Kockrick, L. Borchardt, M. Oschatz, S. Kaskel, G. Yushin, *Small* **2011**, *7*, 1108.
[22] M. Schmirler, T. Knorr, T. Fey, A. Lynen, P. Greil, B. J. M. Etzold, *Carbon* **2011**, *49*, 4359.
[23] P. Colombo, *J. Eur. Ceram. Soc.* **2008**, *28*, 1389.
[24] M. Fukushima, P. Colombo, *J. Eur. Ceram. Soc.* **2012**, *32*, 503.
[25] R. Frind, M. Oschatz, S. Kaskel, *J. Mater. Chem.* **2011**, *21*, 11936.
[26] N. R. Cameron, *Polymer* **2005**, *46*, 1439.
[27] M. Thommes, *Chem. Ing. Tech.* **2010**, *82*, 1059.
[28] A. V. Neimark, Y. Lin, P. I. Ravikovitch, M. Thommes, *Carbon* **2009**, *47*, 1617.
[29] G. Y. Gor, M. Thommes, K. A. Cychosz, A. V. Neimark, *Carbon* **2012**, *50*, 1583.

